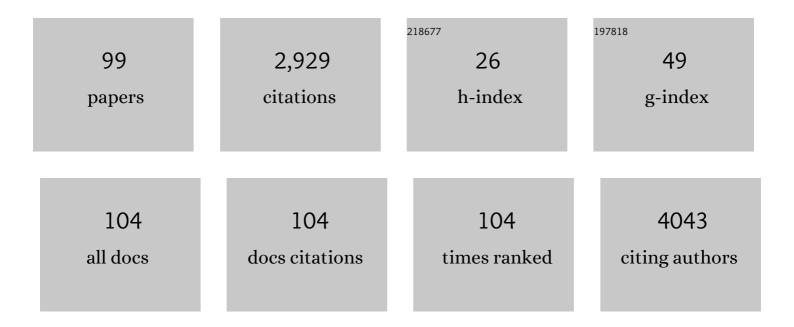
List of Publications by Year in descending order

Source: https://exaly.com/author-pdf/544080/publications.pdf Version: 2024-02-01



Νεζιή Ρλιλ

#	Article	IF	CITATIONS
1	Sonochemistry: Science and Engineering. Ultrasonics Sonochemistry, 2016, 29, 104-128.	8.2	266
2	Prospects and Challenges of Volatile Organic Compound Sensors in Human Healthcare. ACS Sensors, 2018, 3, 1246-1263.	7.8	179
3	Rapid Detection of Infectious Envelope Proteins by Magnetoplasmonic Toroidal Metasensors. ACS Sensors, 2017, 2, 1359-1368.	7.8	158
4	LIGHTNETs: Smart LIGHTing and Mobile Optical Wireless NETworks — A Survey. IEEE Communications Surveys and Tutorials, 2013, 15, 1620-1641.	39.4	136
5	Electrochemical cortisol immunosensors based on sonochemically synthesized zinc oxide 1D nanorods and 2D nanoflakes. Biosensors and Bioelectronics, 2015, 63, 124-130.	10.1	136
6	Exchanging Ohmic Losses in Metamaterial Absorbers with Useful Optical Absorption for Photovoltaics. Scientific Reports, 2014, 4, 4901.	3.3	133
7	loT-based occupancy monitoring techniques for energy-efficient smart buildings. , 2015, , .		132
8	Extreme sensitive metasensor for targeted biomarkers identification using colloidal nanoparticles-integrated plasmonic unit cells. Biomedical Optics Express, 2018, 9, 373.	2.9	116
9	Lactate biosensing: The emerging point-of-care and personal health monitoring. Biosensors and Bioelectronics, 2018, 117, 818-829.	10.1	107
10	Highly Sensitive Wide Bandwidth Photodetector Based on Internal Photoemission in CVD Grown p-Type MoS <sub>2</sub> /Graphene Schottky Junction. ACS Applied Materials & Interfaces, 2015, 7, 15206-15213.	8.0	98
11	Hybrid 3-D Localization for Visible Light Communication Systems. Journal of Lightwave Technology, 2015, 33, 4589-4599.	4.6	81
12	Tunable plasmonic toroidal terahertz metamodulator. Physical Review B, 2018, 97, .	3.2	81
13	Transition from capacitive coupling to direct charge transfer in asymmetric terahertz plasmonic assemblies. Optics Letters, 2016, 41, 5333.	3.3	77
14	AOA-based localization and tracking in multi-element VLC systems. , 2015, , .		58
15	Optical Switching Using Transition from Dipolar to Charge Transfer Plasmon Modes in Ge2Sb2Te5 Bridged Metallodielectric Dimers. Scientific Reports, 2017, 7, 42807.	3.3	57
16	VO <sub>2</sub> â€Based Reconfigurable Antenna Platform with Addressable Microheater Matrix. Advanced Electronic Materials, 2017, 3, 1700170.	5.1	54
17	Magneto-plasmonic nanostars for image-guided and NIR-triggered drug delivery. Scientific Reports, 2020, 10, 10115.	3.3	49
18	Review—A Review of Electrochemical Aptasensors for Label-Free Cancer Diagnosis. Journal of the Electrochemical Society, 2020, 167, 067511.	2.9	48

#	Article	IF	CITATIONS
19	Hot electron generation by aluminum oligomers in plasmonic ultraviolet photodetectors. Optics Express, 2016, 24, 13665.	3.4	45
20	Multi-Element VLC Networks: LED Assignment, Power Control, and Optimum Combining. IEEE Journal on Selected Areas in Communications, 2018, 36, 121-135.	14.0	43
21	Active Control over the Interplay between the Dark and Hidden Sides of Plasmonics Using Metallodielectric Au–Ge <sub>2</sub> Sb <sub>2</sub> Te <sub>5</sub> Unit Cells. Journal of Physical Chemistry C, 2017, 121, 19966-19974.	3.1	42
22	Rhodium Plasmonics for Deep-Ultraviolet Bio-Chemical Sensing. Plasmonics, 2016, 11, 839-849.	3.4	37
23	Enhancement of photothermal heat generation by metallodielectric nanoplasmonic clusters. Optics Express, 2015, 23, A682.	3.4	34
24	Highly sensitive label-free electrochemical aptasensors based on photoresist derived carbon for cancer biomarker detection. Biosensors and Bioelectronics, 2020, 170, 112598.	10.1	32
25	Sonochemical Synthesis of a Zinc Oxide Core–Shell Nanorod Radial p–n Homojunction Ultraviolet Photodetector. ACS Applied Materials & Interfaces, 2017, 9, 19791-19799.	8.0	29
26	Large-Modulation-Depth Polarization-Sensitive Plasmonic Toroidal Terahertz Metamaterial. IEEE Photonics Technology Letters, 2017, 29, 1860-1863.	2,5	28
27	Hybridized plasmon resonant modes in molecular metallodielectric quad-triangles nanoantenna. Optics Communications, 2015, 355, 103-108.	2.1	27
28	Flexible and Linker-Free Enzymatic Sensors Based on Zinc Oxide Nanoflakes for Noninvasive L-Lactate Sensing in Sweat. IEEE Sensors Journal, 2020, 20, 5102-5109.	4.7	27
29	Hybridized plasmons in graphene nanorings for extreme nonlinear optics. Optical Materials, 2017, 73, 729-735.	3.6	26
30	Tunable Room Temperature THz Sources Based on Nonlinear Mixing in a Hybrid Optical and THz Micro-Ring Resonator. Scientific Reports, 2015, 5, 9422.	3.3	22
31	Controlled Synthesis of Singleâ€Crystalline ZnO Nanoflakes on Arbitrary Substrates at Ambient Conditions. Particle and Particle Systems Characterization, 2014, 31, 190-194.	2.3	20
32	Single- and Multimode Beam Propagation Through an Optothermally Controllable Fano Clusters-Mediated Waveguide. Journal of Lightwave Technology, 2017, 35, 4961-4966.	4.6	20
33	A Software-Defined Multi-Element VLC Architecture. , 2018, 56, 196-203.		20
34	A Review of THz Technologies for Rapid Sensing and Detection of Viruses including SARS-CoV-2. Biosensors, 2021, 11, 349.	4.7	20
35	Multiple Step Growth of Single Crystalline Rutile Nanorods with the Assistance of Self-Assembled Monolayer for Dye Sensitized Solar Cells. ACS Applied Materials & Interfaces, 2013, 5, 9809-9815.	8.0	19
36	Slow Beam Steering and NOMA for Indoor Multi-User Visible Light Communications. IEEE Transactions on Mobile Computing, 2021, 20, 1627-1641.	5.8	19

#	Article	IF	CITATIONS
37	Fano resonances in plasmonic aluminum nanoparticle clusters for precise gas detection: Ultra-sensitivity to the minor environmental refractive index perturbations. Photonics and Nanostructures - Fundamentals and Applications, 2015, 13, 97-105.	2.0	18
38	Multi-Element Transmitter Design and Performance Evaluation for Visible Light Communication. , 2015, , .		17
39	Fano Resonances in Complex Plasmonic Necklaces Composed of Gold Nanodisks Clusters for Enhanced LSPR Sensing. IEEE Sensors Journal, 2015, 15, 1588-1594.	4.7	17
40	Tunable THz wave absorption by graphene-assisted plasmonic metasurfaces based on metallic split ring resonators. Journal of Nanoparticle Research, 2017, 19, 1.	1.9	17
41	Functional Quadrumer Clusters for Switching Between Fano and Charge Transfer Plasmons. IEEE Photonics Technology Letters, 2017, 29, 2226-2229.	2.5	16
42	Accuracy of AOA-Based and RSS-Based 3D Localization for Visible Light Communications. , 2015, , .		15
43	Perspectives on C-MEMS and C-NEMS biotech applications. Biosensors and Bioelectronics, 2021, 180, 113119.	10.1	15
44	Magnetic fano resonances in all-dielectric nanocomplexes under cylindrical vector beams excitation. Optics and Laser Technology, 2017, 90, 65-70.	4.6	14
45	Optothermally controllable multiple high-order harmonics generation by Ge2Sb2Te5-mediated Fano clusters. Optical Materials, 2018, 84, 301-306.	3.6	14
46	Graphene Optical Switch Based on Charge Transfer Plasmons. Physica Status Solidi - Rapid Research Letters, 2017, 11, 1700285.	2.4	13
47	Selective Detection of Alcohol Through Ethyl-Glucuronide Immunosensor Based on 2D Zinc Oxide Nanostructures. IEEE Sensors Journal, 2019, 19, 3984-3992.	4.7	13
48	Insights on cholinium- and piperazinium-based ionic liquids under external electric fields: A molecular dynamics study. Journal of Chemical Physics, 2013, 139, 224502.	3.0	12
49	Localization, Hybridization, and Coupling of Plasmon Resonances in an Aluminum Nanomatryushka. Plasmonics, 2015, 10, 809-817.	3.4	12
50	Design Rules for a Wearable Micro-Fabricated Piezo-Resistive Pressure Sensor. Micromachines, 2022, 13, 838.	2.9	12
51	Tunable, Room Temperature CMOS-Compatible THz Emitters Based on Nonlinear Mixing in Microdisk Resonators. Journal of Infrared, Millimeter, and Terahertz Waves, 2016, 37, 230-242.	2.2	11
52	Highly Sensitive Lactic Acid Biosensors Based on Photoresist Derived Carbon. IEEE Sensors Journal, 2020, 20, 8965-8972.	4.7	11
53	VO2-based ultra-reconfigurable intelligent reflective surface for 5G applications. Scientific Reports, 2022, 12, 4497.	3.3	11
54	Deep Sub-Wavelength Multimode Tunable In-Plane Plasmonic Lenses Operating at Terahertz Frequencies. IEEE Transactions on Terahertz Science and Technology, 2013, 3, 550-557.	3.1	10

5

#	Article	IF	CITATIONS
55	Fano-Like Resonances in Split Concentric Nanoshell Dimers in Designing Negative-Index Metamaterials for Biological-Chemical Sensing and Spectroscopic Purposes. Applied Spectroscopy, 2015, 69, 563-573.	2.2	10
56	Intensifying magnetic dark modes in the antisymmetric plasmonic quadrumer composed of Al/Al 2 O 3 nanodisks with the placement of silicon nanospheres. Optics Communications, 2015, 338, 218-225.	2.1	10
57	Excitation of Terahertz Charge Transfer Plasmons in Metallic Fractal Structures. Journal of Infrared, Millimeter, and Terahertz Waves, 2017, 38, 992-1003.	2.2	10
58	Plasmonic properties of asymmetric dual grating gate plasmonic crystals. Physica Status Solidi (B): Basic Research, 2016, 253, 671-675.	1.5	9
59	\$hbox{HfO}_{2}\$–III-Nitride RF Switch With Capacitively Coupled Contacts. IEEE Electron Device Letters, 2009, 30, 478-480.	3.9	8
60	Plasmon Resonance Hybridization in Self-Assembled Copper Nanoparticle Clusters: Efficient and Precise Localization of Surface Plasmon Resonance (LSPR) Sensing Based on Fano Resonances. Applied Spectroscopy, 2015, 69, 277-286.	2.2	8
61	Multiple coil-type Fano resonances in all-dielectric antisymmetric quadrumers. Optical and Quantum Electronics, 2015, 47, 2055-2064.	3.3	8
62	Diversity combining and piezoelectric beam steering for multi-element VLC networks. , 2016, , .		8
63	A molecular plasmonic Fano-router: Using hotspots in a single-stone ring-like structure. Optics Communications, 2016, 367, 123-129.	2.1	8
64	Al-Powered Terahertz VLSI Testing Technology for Ensuring Hardware Security and Reliability. IEEE Access, 2021, 9, 64499-64509.	4.2	8
65	Plasmon response of a metal-semiconductor multilayer 4Ï€-spiral as a negative-index metamaterial. Journal of Nanoparticle Research, 2014, 16, 1.	1.9	7
66	Fano Resonances in Nanoshell Clusters Deposited on a Multilayer Substrate of \$meta\$-SiC/SiO <sub>2</sub> /Si to Design High-Quality Plasmonic Sensors. Journal of Lightwave Technology, 2015, 33, 2817-2823.	4.6	7
67	Novel application of electrochemical bipolar exfoliated graphene for highly sensitive disposable label-free cancer biomarker aptasensors. Nanoscale Advances, 2021, 3, 5948-5958.	4.6	7
68	Resonance coupling in plasmonic nanomatryoshka homo- and heterodimers. AIP Advances, 2016, 6, .	1.3	6
69	Graphene-Based Periodic Gate Field Effect Transistor Structures for Terahertz Applications. Nanoscience and Nanotechnology Letters, 2013, 5, 754-757.	0.4	6
70	In-Situ Integration of 3D C-MEMS Microelectrodes with Bipolar Exfoliated Graphene for Label-Free Electrochemical Cancer Biomarkers Aptasensor. Micromachines, 2022, 13, 104.	2.9	6
71	A Facile Fabrication of Porous and Breathable Dielectric Film for Capacitive Pressure Sensor. , 2020, , .		6

72 A Multi-Element VLC Architecture for High Spatial Reuse. , 2015, , .

#	Article	IF	CITATIONS
73	Analyzing Photothermal Heat Generation Efficiency in a Molecular Plasmonic Silver Nanomatryushka Dimer. Plasmonics, 2016, 11, 493-501.	3.4	5
74	Absorption Enhancement in Ultrathin Structures Based on Crystalline-Si/Ag Parabola Nanocones Periodic Arrays with Broadband Antireflection Property. Silicon, 2017, 9, 25-29.	3.3	5
75	Al Powered THz Testing Technology for Ensuring Hardware Cybersecurity. , 2020, , .		5
76	Additive manufacturing of borosilicate glass via stereolithography. Ceramics International, 2022, 48, 12721-12728.	4.8	5
77	Implantable Devices for the Treatment of Breast Cancer. Journal of Nanotheranostics, 2022, 3, 19-38.	3.1	5
78	Improving High-Frequency Characteristics of Graphene FETs by Field-Controlling Electrodes. IEEE Electron Device Letters, 2013, 34, 1193-1195.	3.9	4
79	Sonochemically Synthesized ZnO Nanostructure-Based L-Lactate Enzymatic Sensors on Flexible Substrates. MRS Advances, 2018, 3, 277-282.	0.9	4
80	Synthesis of Crystalline ZnO Nanosheets on Graphene and Other Substrates at Ambient Conditions. Materials Research Society Symposia Proceedings, 2012, 1449, 121.	0.1	3
81	Electromagnetic wave propagation along T and Y-splitters composed of silicon nanorods, gold slots, and silica substrate. Optics Communications, 2015, 343, 73-79.	2.1	3
82	Selfâ€assembled siliconâ€based clusters to design efficient, fast, and controllable Fano switches. Microwave and Optical Technology Letters, 2015, 57, 1242-1246.	1.4	3
83	Graphene FETs with Low-Resistance Hybrid Contacts for Improved High Frequency Performance. Nanomaterials, 2016, 6, 86.	4.1	3
84	Bandgap engineering of single layer graphene by randomly distributed nanoparticles. Journal of Materials Science: Materials in Electronics, 2016, 27, 7454-7459.	2.2	3
85	ZnO Nanoflakes based Enzymatic Sensor for the determination of lactic acid in sweat. , 2019, , .		3
86	Multiple Fano Resonances in Plasmonic Metamaterials Composed of Al/Al2O3 Nanomatryushka Structures. Materials Research Society Symposia Proceedings, 2015, 1788, 43-48.	0.1	2
87	THz Detectors. , 2016, , 373-414.		2
88	Sonochemically Synthesized Zinc Oxide Nanoflakes Based Electrochemical Immunosensor for Ethyl Glucuronide (EtG) Detection. ECS Transactions, 2017, 80, 1287-1294.	0.5	2
89	Optothermally Controlled Charge Transfer Plasmons in Au-Ge2Sb2Te5 Core-Shell Dimers. Plasmonics, 2018, 13, 1921-1928.	3.4	2

90 Hybrid Toroidal Modes in Planar Core-Shell Metamaterial Structures., 2018,,.

2

#	Article	IF	CITATIONS
91	Silicon Nanowire Integrated Electrolyte-Insulator-Semiconductor Sensor with an Above-Nernstian Sensitivity for Bio-Sensing Applications. Materials Research Society Symposia Proceedings, 2012, 1439, 127-132.	0.1	1
92	Ultraviolet LED based compact and fast cortisol detector with ultra high sensitivity. , 2016, , .		1
93	Hybrid Toroidal Resonance Response in Planar Core-Shell THz Metasurfaces. Plasmonics, 2021, 16, 1657-1663.	3.4	1
94	Silicon nanorodsâ€based allâ€dielectric waveguides with long decayâ€length at the telecommunication band. International Journal of Numerical Modelling: Electronic Networks, Devices and Fields, 2016, 29, 530-543.	1.9	0
95	Optothermally Tuned Charge Transfer Plasmons in Au-Ge2Sb2Te5 Core-Shell Assemblies. MRS Advances, 2018, 3, 1919-1924.	0.9	0
96	Performance Evaluation of Liquid 3D Chip Cooling Systems Under Non-Uniform Power Density: Effects of Inlet and Plenum Configurations. , 2019, , .		0
97	Sonochemically Synthesized ZnO Nanostructured Piezoelectric Layers for Self-Powered Sensor Applications. MRS Advances, 2019, 4, 1355-1360.	0.9	0
98	Highly Tunable, Flexible and Stretchable Frequency Selective Surface-Based THz Bandpass Filter. , 2019, , .		0
99	Raman Signal Amplification in Photonic Crystal Microring Resonators. , 2019, , .		0